The generalized plane strain deformations of thick anisotropic composite laminated plates

Senthil S. Vel, R.C. Batra*

Department of Engineering Science and Mechanics, MC-0219, Virginia Polytechnic Institute and State University, Blacksburg, VA 24061, USA

Abstract

We use the Eshelby–Stroh formalism to analyze the generalized plane strain quasistatic deformations of an anisotropic, linear elastic laminated plate. The laminate consists of homogeneous laminae of arbitrary thicknesses. Computed results are presented for three sample problems to illustrate the effect of boundary conditions and of the span to height ratio. © 1999 Elsevier Science Ltd. All rights reserved.

Keywords: Analytical solution; Cylindrical bending; Clamped edges; Eshelby–Stroh formalism

1. Introduction

Pagano (1969, 1970) used the linear elasticity theory to analyze quasistatic deformations of an orthotropic simply supported laminated plate under the assumption of generalized plane strain deformations and compared his results with those obtained by using the classical plate theory. Meleshko (1997) has recently reviewed the history and strategies for finding analytically displacements and stresses in a clamped-clamped thin plate of arbitrary length to width ratio. As is clear from Meleshko's paper, there has been significant interest in finding an analytical solution of the nonhomogeneous biharmonic equation for boundary conditions simulating clamped edges; a biharmonic equation models bending deformations of a thin plate. We refer the reader to Meleshko (1997), Kapania and Raciti (1989), Noor and Burton (1989), Soldatos and Watson (1997), Jones (1975) and Reddy (1997) for a historical perspective and for a review of various approximate plate theories. As far as we can ascertain, the challenging problem of finding an analytical solution of the linear elasticity equations governing deformations of a

---

* Corresponding author. Tel.: +1-540-231-6051; fax: +1-540-231-4574.
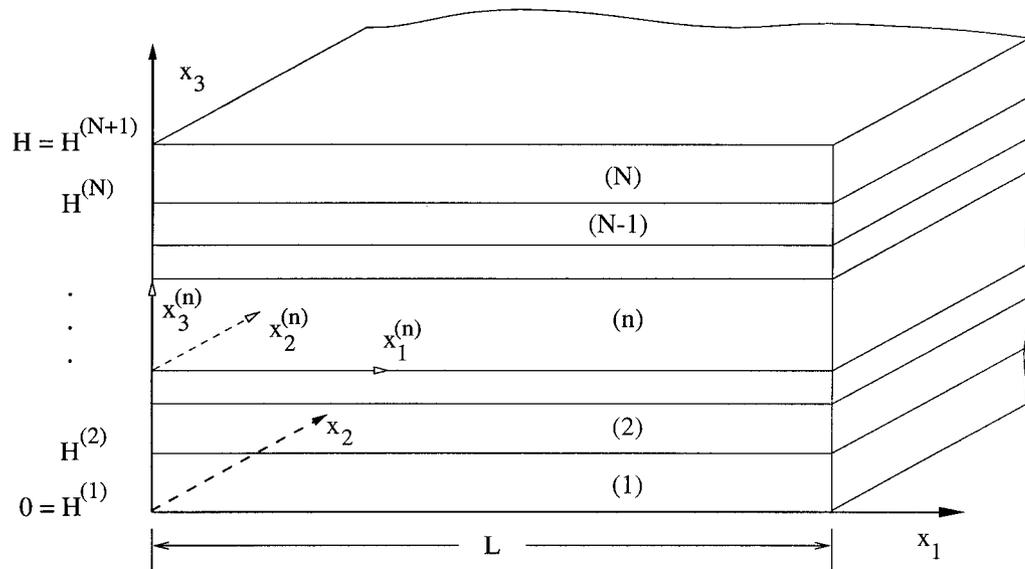 *E-mail address:* rbatra@vt.edu (R.C. Batra)

Fig. 1. An *N*-layer elastic plate.

clamped-clamped plate of arbitrary span to thickness ratio remains unsolved[1]. Here we present an analytical solution of the cylindrical bending of a clamped-clamped, anisotropic, linear elastic plate of arbitrary span to thickness ratio. As illustrated by results for clamped-free, and clamped-simply supported laminates, our formulation admits different boundary conditions. Three-dimensional equations of linear elasticity simplified to the case of generalized plane-strain deformations are solved by the Eshelby–Stroh formalism. Thus the governing equations are exactly satisfied, and various constants in the general solution are determined from the boundary and the continuity conditions at the interfaces. This results in an infinite system of equations in infinitely many unknowns. The truncation of this set of equations inevitably involves some errors which can be minimized by increasing the number of terms in the series. The procedure is illustrated by computing results for the cylindrical bending of a plate of arbitrary span to thickness ratio and either rigidly clamped at both edges or clamped at one end and simply supported at the other. These results should help others compare approximate plate theories with the analytical solution and thus assess the accuracy of their proposed plate theories.

2. Formulation of the problem

We use a rectangular Cartesian coordinate system, shown in Fig. 1, to describe the infinitesimal quasistatic deformations of an *N*-layer anisotropic elastic laminate occupying the region $[0, L] \times (-\infty, \infty) \times [H^{(1)}, H^{(N + 1)}]$ in the unstressed reference configuration. Planes $x_3 = H^{(1)}, H^{(2)}, \ldots, H^{(n)}, \ldots, H^{(N + 1)}$ describe, respectively, the lower bounding surface, the interface between the bottom-most and the adjoining lamina, the interfaces between abutting laminae, and the top bounding surface. Equations governing

---

[1] The authors found Srinivas and Rao's (1973) technical note subsequent to the submission of the final manuscript. The technique presented here is more general than that given by Srinivas and Rao (1973).

the displacements $\mathbf{u} = \mathbf{x} - \mathbf{X}$ of a material point $\mathbf{X}$ are

$$\sigma_{ij,\, j} = 0, \quad (i, j = 1, 2, 3), \tag{1}$$

$$\sigma_{ij} = C_{ijkl} u_{k,\, l}, \tag{2}$$

$$C_{ijkl} = C_{jikl} = C_{klij}. \tag{3}$$

Here $\mathbf{x}$ is the present position of the material particle that occupied place $\mathbf{X}$ in the reference configuration, σ_{ij} is the Cauchy stress tensor, C_{ijkl} are elastic constants, a comma followed by index j indicates partial differentiation with respect to x_j, and a repeated index implies summation over the range of the index. We will interchangeably use the direct and indicial notation. Material elasticities are assumed to yield a positive strain energy density for every non-rigid deformation of the body.

The displacement or traction components prescribed on the side surfaces $x_1 = 0, L$ and the bottom and top surfaces $x_3 = H^{(1)}$, $H^{(N + 1)}$ are presumed not to depend upon x_2, and are specified as follows (e.g. see Ting, 1996, p. 498)

$$\mathbf{I}_u^l \mathbf{u} + \mathbf{I}_\sigma^l \boldsymbol{\sigma}_1 = \mathbf{g}^l(x_3) \quad \text{on} \quad x_1 = 0,$$

$$\mathbf{I}_u^r \mathbf{u} + \mathbf{I}_\sigma^r \boldsymbol{\sigma}_1 = \mathbf{g}^r(x_3) \quad \text{on} \quad x_1 = L,$$

$$\mathbf{I}_u^b \mathbf{u} + \mathbf{I}_\sigma^b \boldsymbol{\sigma}_3 = \mathbf{g}^b(x_1) \quad \text{on} \quad x_3 = H^{(1)},$$

$$\mathbf{I}_u^t \mathbf{u} + \mathbf{I}_\sigma^t \boldsymbol{\sigma}_3 = \mathbf{g}^t(x_1) \quad \text{on} \quad x_3 = H^{(N+1)}, \tag{4}$$

where

$$(\boldsymbol{\sigma}_1)_i = \sigma_{i1}, \quad (\boldsymbol{\sigma}_3)_i = \sigma_{i3}. \tag{5}$$

The functions $\mathbf{g}^l(x_3)$, $\mathbf{g}^r(x_3)$, $\mathbf{g}^b(x_1)$ and $\mathbf{g}^t(x_1)$ are known, while $\mathbf{I}_u^l$, $\mathbf{I}_\sigma^l$, $\mathbf{I}_u^r$, $\mathbf{I}_\sigma^r$, $\mathbf{I}_u^b$, $\mathbf{I}_\sigma^b$, $\mathbf{I}_u^t$ and $\mathbf{I}_\sigma^t$ are 3×3 diagonal matrices whose elements are constants. For most applications, these matrices are diagonal with entries either zero or one such that

$$\mathbf{I}_u^l + \mathbf{I}_\sigma^l = \mathbf{I}_u^r + \mathbf{I}_\sigma^r = \mathbf{I}_u^b + \mathbf{I}_\sigma^b = \mathbf{I}_u^t + \mathbf{I}_\sigma^t = \mathbf{I} \tag{6}$$

with $\mathbf{I}$ being the 3×3 identity matrix. For example, if the surface $x_1 = 0$ is rigidly clamped, then $\mathbf{I}_u^l = \mathbf{I}$, $\mathbf{I}_\sigma^l = \mathbf{0}$ and $\mathbf{g}^l(x_3) = \mathbf{0}$. However, if it is simply supported, then $\mathbf{I}_u^l = \text{diag}[0, 1, 1]$, $\mathbf{I}_\sigma^l = \text{diag}[1, 0, 0]$ and $\mathbf{g}^l(x_3) = \mathbf{0}$. Thus at the simply supported edge $u_2 = u_3 = 0$, $\sigma_{11} = 0$. These boundary conditions are identical to those used by Pagano (1969) at a simply supported edge. For a laminate on an elastic foundation, the matrices $\mathbf{I}_u^b$, $\mathbf{I}_\sigma^b$, $\mathbf{I}_u^t$ and $\mathbf{I}_\sigma^t$ may not satisfy (6); such boundary conditions will be studied elsewhere. The interfaces between different laminae are assumed to be perfectly bonded together. Thus displacements and surface tractions between the adjoining laminae are taken to be continuous which may be stated as

$$[\![\mathbf{u}]\!] = \mathbf{0}, \ [\![\boldsymbol{\sigma}_3]\!] = \mathbf{0} \quad \text{on} \quad x_3 = H^{(2)}, H^{(3)}, \ldots, H^{(N)}. \tag{7}$$

Here $[\![\mathscr{F}]\!]$ denotes the jump in the value of $\mathscr{F}$ across an interface.

We postulate that the displacement $\mathbf{u}$ is a function of x_1 and x_3 only and thus the deformations of the laminate correspond to generalized plane strain state of deformation. This assumption is reasonable

since the applied loads are independent of x_2, the body is of infinite extent in the x_2 direction, and elasticities are constants.

3. Solution of the problem

We use the Eshelby–Stroh (Eshelby et al., 1953; Stroh, 1958) formalism as described by Ting (1996) to obtain a general solution of Eqs. (1)–(3). Boundary conditions (4) and interface conditions (7) will be used to find constants in the general solution. We construct a local coordinate system $x_1^{(n)}$, $x_2^{(n)}$, $x_3^{(n)}$ with origin at the point where the global x_3 axis intersects the bottom surface of the nth lamina; the local axes are parallel to the global axes. The thickness of the nth lamina is denoted by $h^{(n)} = H^{(n+1)} - H^{(n)}$.

3.1. A general solution

In deriving a general solution of Eqs. (1)–(3) for the nth lamina, we drop the superscript n, it being understood that all material constants and variables belong to this lamina. Assume that

$$\mathbf{u} = \mathbf{a}f(z), \quad z = x_1 + px_3, \tag{8}$$

where f is an arbitrary analytic function of z, and $\mathbf{a}$ and p are possible complex constants to be determined. Substitution of (8) into (2) and the result into (1) gives

$$\{\mathbf{Q} + p(\mathbf{R} + \mathbf{R}^{\mathrm{T}}) + p^2\mathbf{T}\}\mathbf{a} = \mathbf{0}, \tag{9}$$

where $Q_{ik} = C_{i1k1} = Q_{ki}$, $R_{ik} = C_{i1k3}$, and $T_{ik} = C_{i3k3} = T_{ki}$ are 3×3 matrices. The positive-definiteness of the strain energy density implies that $\mathbf{Q}$ and $\mathbf{T}$ are positive definite matrices. We rewrite the eigenvalue problem (9) as

$$\mathbf{N}\boldsymbol{\zeta} = p\boldsymbol{\zeta} \tag{10}$$

where

$$\mathbf{N} = \begin{bmatrix} -\mathbf{T}^{-1}\mathbf{R}^{\mathrm{T}} & \mathbf{T}^{-1} \\ \mathbf{R}\mathbf{T}^{-1}\mathbf{R}^{\mathrm{T}} - \mathbf{Q} & -\mathbf{R}\mathbf{T}^{-1} \end{bmatrix}, \quad \boldsymbol{\zeta} = \begin{Bmatrix} \mathbf{a} \\ \mathbf{b} \end{Bmatrix}, \tag{11}$$

$$\mathbf{b} = -\frac{1}{p}(\mathbf{Q} + p\mathbf{R})\mathbf{a} = (\mathbf{R}^{\mathrm{T}} + p\mathbf{T})\mathbf{a}. \tag{12}$$

Therefore, p is a root of

$$\det[\mathbf{N} - p\mathbf{I}] = 0, \tag{13}$$

and then the eigenvector $\boldsymbol{\zeta}$ and hence $\mathbf{a}$, $\mathbf{b}$ can be determined from (10)–(11). The 6×6 matrix $\mathbf{N}$ is called the *fundamental elasticity matrix*. For the strain energy density to be positive definite, p must be complex (Eshelby et al., 1953). Let $(p_\alpha, \mathbf{a}_\alpha)$, $(\alpha = 1, 2, \ldots, 6)$ be eigensolutions of (9) such that

$$\mathrm{Im}(p_\alpha) > 0, \quad p_{\alpha+3} = \bar{p}_\alpha, \quad \mathbf{a}_{\alpha+3} = \bar{\mathbf{a}}_\alpha, \quad (\alpha = 1, 2, 3), \tag{14}$$

where a bar superimposed on a quantity denotes its complex conjugate. Assuming that p's are distinct, a general solution of (1)–(3) obtained by superposing six solutions of the form (8) is

$$\mathbf{u} = \sum_{\alpha=1}^{3}[\mathbf{a}_\alpha f_\alpha(z_\alpha) + \bar{\mathbf{a}}_\alpha f_{\alpha+3}(\bar{z}_\alpha)], \tag{15}$$

where f_α ($\alpha = 1, 2, \ldots, 6$) are arbitrary analytic functions and $z_\alpha = x_1 + p_\alpha x_3$. Substitution from (15) into (2), and the result into (5) yields

$$\boldsymbol{\sigma}_1 = -\sum_{\alpha=1}^{3}[p_\alpha \mathbf{b}_\alpha f'_\alpha(z_\alpha) + \bar{p}_\alpha \bar{\mathbf{b}}_\alpha f'_{\alpha+3}(\bar{z}_\alpha)],$$

$$\boldsymbol{\sigma}_3 = \sum_{\alpha=1}^{3}[\mathbf{b}_\alpha f'_\alpha(z_\alpha) + \bar{\mathbf{b}}_\alpha f'_{\alpha+3}(\bar{z}_\alpha)], \tag{16}$$

where $f'(z) = \mathrm{d}f(z)/\mathrm{d}z$. Vectors $\mathbf{a}_\alpha$ and $\mathbf{b}_\alpha$ are called the Stroh eigenvectors. As noted by Ting (1996), once the eigenvalues and eigenvectors are determined the elastic constants C_{ijkl} are no longer needed. Thus (p_α, $\mathbf{a}_\alpha$, $\mathbf{b}_\alpha$), ($\alpha = 1, 2, 3$) although complex can be considered as material constants that determine the generalized plane strain state of deformation.

The general solution (15)–(16) is valid when $\mathbf{N}$ is simple or semisimple, that is, the eigenvalues p_α are distinct or, if not, there exist six independent eigenvectors $\boldsymbol{\zeta}_\alpha$. $\mathbf{N}$ is nonsemisimple for isotropic and certain anisotropic materials. Ting (1982) has discussed how to modify the general solution for nonsemisimple $\mathbf{N}$.

3.2. A series solution

Even though (15) satisfies the equilibrium Eqs. (1)–(3) for all choices of the analytic functions f_α, a choice based on the geometry of the problem and boundary conditions can simplify the algebraic details. We select for the nth lamina

$$f_\alpha^{(n)}(z_\alpha^{(n)}) = d_\alpha^{(n)} + z_\alpha^{(n)} v_\alpha^{(n)} + (z_\alpha^{(n)})^2 w_\alpha^{(n)} + \sum_{k=1}^{\infty}\{q_{k\alpha}^{(n)} \exp(\lambda_{k\alpha}^{(n)} z_\alpha^{(n)}) + r_{k\alpha}^{(n)} \exp(\lambda_{k\alpha}^{(n)}(p_\alpha^{(n)} h^{(n)} - z_\alpha^{(n)}))\}$$

$$+ \sum_{m=1}^{\infty}\{s_{m\alpha}^{(n)} \exp(\eta_{m\alpha}^{(n)} z_{m\alpha}^{(n)}) + t_{m\alpha}^{(n)} \exp(\eta_{m\alpha}^{(n)}(L - z_\alpha^{(n)}))\}, \quad 0 \le x_3^{(n)} \le h^{(n)},$$

$$f_{\alpha+3}^{(n)}(\bar{z}_\alpha^{(n)}) = \overline{f_\alpha^{(n)}(z_\alpha^{(n)})}, \tag{17}$$

where $z_\alpha^{(n)} = x_1^{(n)} + p_\alpha^{(n)} x_3^{(n)}$,

$$\lambda_{k\alpha}^{(n)} = \frac{k\pi i}{L}, \quad \eta_{m\alpha}^{(n)} = -\frac{m\pi i}{p_\alpha^{(n)} h^{(n)}}, \quad i = \sqrt{-1}. \tag{18}$$

The unknowns $d_\alpha^{(n)}$ and $w_\alpha^{(n)}$ are assumed to be real while $v_\alpha^{(n)}$, $q_{k\alpha}^{(n)}$, $r_{k\alpha}^{(n)}$, $s_{m\alpha}^{(n)}$ and $t_{m\alpha}^{(n)}$ are complex; these will be determined from the boundary conditions. Note that each term in series (17) is an analytical function of $z_\alpha^{(n)}$. The function $\exp(\lambda_{k\alpha}^{(n)} z_\alpha^{(n)})$ varies sinusoidally on the surface $x_3^{(n)} = 0$ and decays exponentially in the $x_3^{(n)}$-direction. With increasing k, higher harmonics are introduced on the surface $x_3^{(n)} = 0$ accompanied by steeper exponential decay in the $x_3^{(n)}$-direction. Similarly, functions multiplying $r_{k\alpha}^{(n)}$, $s_{m\alpha}^{(n)}$ and $t_{m\alpha}^{(n)}$ vary sinusoidally on surfaces $x_3^{(n)} = h^{(n)}$, $x_1^{(n)} = 0$ and $x_1^{(n)} = L$, respectively. The inequality (14)$_1$ ensures that all functions decay exponentially towards the interior of the layer. The poly-

nomial terms in $z_\alpha^{(n)}$ are introduced to play the role of the constant in the Fourier series expansion on the four bounding surfaces. The choice $f_{\alpha+3}^{(n)}(\bar{z}_\alpha^{(n)})$ equal to the complex conjugate of $f_\alpha^{(n)}(z_\alpha^{(n)})$ ensures that displacements and stresses are real.

Pagano (1969) studied quasistatic deformations of a simply supported laminate subjected to a sinusoidal load on the upper and/or lower long faces. His series solution identically satisfies the boundary conditions at the edges. We have included additional terms, represented by the infinite series with index m in (17), to satisfy all types of boundary conditions and to capture boundary layer effects, if any, near the edges. Both Pagano's series solution and our solution (17) seem to be complete; neither he proved it nor we prove this very challenging problem. Substitution from (17) into (15) and (16) results in the following expressions

$$\mathbf{u}^{(n)} = \mathbf{A}^{(n)} \left\{ \mathbf{d}^{(n)} + \langle z_*^{(n)} \rangle \mathbf{v}^{(n)} + \langle (z_*^{(n)})^2 \rangle \mathbf{w}^{(n)} + \sum_{k=1}^{\infty} [\langle \exp(\beta_{k*}^{(n)}) \rangle \mathbf{q}_k^{(n)} + \langle \exp(\gamma_{k*}^{(n)}) \rangle \mathbf{r}_k^{(n)}] \right.$$
$$\left. + \sum_{m=1}^{\infty} [\langle \exp(\delta_{m*}^{(n)}) \rangle \mathbf{s}_m^{(n)} + \langle \exp(\xi_{m*}^{(n)}) \rangle \mathbf{t}_m^{(n)}] \right\} + \text{conjugate}, \tag{19}$$

$$\boldsymbol{\sigma}_1^{(n)} = \mathbf{B}^{(n)} \left\{ -\langle p_*^{(n)} \rangle \mathbf{v}^{(n)} - \langle 2p_*^{(n)} z_*^{(n)} \rangle \mathbf{w}^{(n)} + \sum_{k=1}^{\infty} [-\langle \lambda_{k*}^{(n)} p_*^{(n)} \exp(\beta_{k*}^{(n)}) \rangle \mathbf{q}_k^{(n)} + \langle \lambda_{k*}^{(n)} p_*^{(n)} \exp(\gamma_{k*}^{(n)}) \rangle \mathbf{r}_k^{(n)}] \right.$$
$$\left. + \sum_{m=1}^{\infty} [-\langle \eta_{m*}^{(n)} p_*^{(n)} \exp(\delta_{m*}^{(n)}) \rangle \mathbf{s}_m^{(n)} + \langle \eta_{m*}^{(n)} p_*^{(n)} \exp(\xi_{m*}^{(n)}) \rangle \mathbf{t}_m^{(n)}] \right\} + \text{conjugate}, \tag{20}$$

$$\boldsymbol{\sigma}_3^{(n)} = \mathbf{B}^{(n)} \left\{ \mathbf{v}^{(n)} + \langle 2z_*^{(n)} \rangle \mathbf{w}^{(n)} + \sum_{k=1}^{\infty} [\langle \lambda_{k*}^{(n)} \exp(\beta_{k*}^{(n)}) \rangle \mathbf{q}_k^{(n)} - \langle \lambda_{k*}^{(n)} \exp(\gamma_{k*}^{(n)}) \rangle \mathbf{r}_k^{(n)}] \right.$$
$$\left. + \sum_{m=1}^{\infty} [\langle \eta_{m*}^{(n)} \exp(\delta_{m*}^{(n)}) \rangle \mathbf{s}_m^{(n)} - \langle \eta_{m*}^{(n)} \exp(\xi_{m*}^{(n)}) \rangle \mathbf{t}_m^{(n)}] \right\} + \text{conjugate}, \tag{21}$$

where

$$\beta_{k\alpha}^{(n)} = \lambda_{k\alpha}^{(n)} z_\alpha^{(n)}, \quad \gamma_{k\alpha}^{(n)} = \lambda_{k\alpha}^{(n)}(p_\alpha^{(n)} h^{(n)} - z_\alpha^{(n)}),$$

$$\delta_{m\alpha}^{(n)} = \eta_{m\alpha}^{(n)} z_\alpha^{(n)}, \quad \xi_{m\alpha}^{(n)} = \eta_{m\alpha}^{(n)}(L - z_\alpha^{(n)}),$$

$$\mathbf{A}^{(n)} = [\mathbf{a}_1^{(n)}, \mathbf{a}_2^{(n)}, \mathbf{a}_3^{(n)}], \quad \mathbf{B}^{(n)} = [\mathbf{b}_1^{(n)}, \mathbf{b}_2^{(n)}, \mathbf{b}_3^{(n)}],$$

$$\langle \phi_* \psi_* \eta_* \rangle = \text{diag}[\phi_1 \psi_1 \eta_1, \phi_2 \psi_2 \eta_2, \phi_3 \psi_3 \eta_3],$$

$$(\mathbf{d}^{(n)})_\alpha = d_\alpha^{(n)}, \quad \alpha = 1, 2, 3. \tag{22}$$

The other unknowns $\mathbf{v}^{(n)}$, $\mathbf{w}^{(n)}$, $\mathbf{q}_k^{(n)}$, $\mathbf{r}_k^{(n)}$, $\mathbf{s}_m^{(n)}$ and $\mathbf{t}_m^{(n)}$ are defined in a way similar to $\mathbf{d}^{(n)}$, and conjugate stands for the complex conjugate of the explicity stated terms.

4. Satisfaction of boundary and interface conditions

The boundary conditions (4) on the surfaces $x_1 = 0$, L; $x_3 = H^{(1)}$, $H^{(N+1)}$, and continuity conditions (7) on the surface $x_3 = H^{(2)}$, $H^{(3)}$, ..., $H^{(N)}$ are satisfied by the classical Fourier series method, resulting in a system of linear equations for the unknown coefficients $\mathbf{d}^{(n)}$, $\mathbf{v}^{(n)}$, $\mathbf{w}^{(n)}$, $\mathbf{q}_k^{(n)}$, $\mathbf{r}_k^{(n)}$, $\mathbf{s}_m^{(n)}$ and $\mathbf{t}_m^{(n)}$.

On the top surface $x_3^{(N)} = h^{(N)}$, we extend the component functions in (19)–(21) over the interval $(-L, 0)$ in the x_1-direction. The sinusoidal functions multiplying $\mathbf{q}_k^{(N)}$ and $\mathbf{r}_k^{(N)}$ are extended without modification since they form the basis functions on this surface. The polynomial and exponential functions corresponding to $\mathbf{d}^{(N)}$, $\mathbf{v}^{(N)}$, $\mathbf{w}^{(N)}$ and $\mathbf{s}_m^{(N)}$, $\mathbf{t}_m^{(N)}$, respectively, are extended as even functions. The prescribed function $\mathbf{g}^t(x_1)$ is suitably extended. It should be noted that these extensions are not unique. We multiply $(4)_4$ by $\exp(j\pi i x_1/L)$ and integrate with respect to x_1 from $-L$ to L to obtain

$$\int_{-L}^{L} \{\mathbf{I}_u^t \mathbf{u}^{(N)}(x_1, h^{(N)}) + \mathbf{I}_\sigma^t \boldsymbol{\sigma}_3^{(N)}(x_1, h^{(N)}) - \mathbf{g}^t(x_1)\} \exp\left(j\frac{i\pi x_1}{L}\right) \mathrm{d}x_1 = \mathbf{0}, \quad j = 0, 1, 2, \ldots \tag{23}$$

The same procedure is repeated for the boundary condition $(4)_3$ on the bottom surface and the interface conditions (7), leading to the following set of equations

$$\int_{-L}^{L} \{\mathbf{I}_u^b \mathbf{u}^{(1)}(x_1, 0) + \mathbf{I}_\sigma^b \boldsymbol{\sigma}_3^{(1)}(x_1, 0) - \mathbf{g}^b(x_1)\} \exp\left(j\frac{i\pi x_1}{L}\right) \mathrm{d}x_1 = \mathbf{0}, \quad j = 0, 1, 2, \ldots,$$

$$\left.\begin{aligned}
\int_{-L}^{L} \{\mathbf{u}^{(n)}(x_1, h^{(n)}) - \mathbf{u}^{(n+1)}(x_1, 0)\} \exp\left(j\frac{i\pi x_1}{L}\right) \mathrm{d}x_1 &= \mathbf{0}, \\
\int_{-L}^{L} \{\boldsymbol{\sigma}_3^{(n)}(x_1, h^{(n)}) - \boldsymbol{\sigma}_3^{(n+1)}(x_1, 0)\} \exp\left(j\frac{i\pi x_1}{L}\right) \mathrm{d}x_1 &= \mathbf{0}.
\end{aligned}\right\} \quad n = 1, 2, \ldots, N-1, \quad j = 0, 1, 2, \ldots \tag{24}$$

Similarly, for the side surfaces $x_1^{(n)} = 0$, L, the functions are extended over the interval $(-h^{(n)}, 0)$ in the $x_3^{(n)}$ direction. The integrations are performed with respect to $x_3^{(n)}$ from $-h^{(n)}$ to $h^{(n)}$ after multiplying $(4)_{1,2}$ by $\exp(j\pi i x_3^{(n)}/h^{(n)})$. We thus obtain

$$\left.\begin{aligned}
\int_{-h(n)}^{h(n)} \{\mathbf{I}_u^l \mathbf{u}^{(n)}(0, x_3^{(n)}) + \mathbf{I}_\sigma^l \boldsymbol{\sigma}_1^{(n)}(0, x_3^{(n)}) - \mathbf{g}^l(x_3^{(n)})\} \exp\left(j\frac{i\pi x_3^{(n)}}{h^{(n)}}\right) \mathrm{d}x_3^{(n)} &= \mathbf{0}, \\
\int_{-h(n)}^{h(n)} \{\mathbf{I}_u^r \mathbf{u}^{(n)}(L, x_3^{(n)}) + \mathbf{I}_\sigma^r \boldsymbol{\sigma}_1^{(n)}(L, x_3^{(n)}) - \mathbf{g}^r(x_3^{(n)})\} \exp\left(j\frac{i\pi x_3^{(n)}}{h^{(n)}}\right) \mathrm{d}x_3^{(n)} &= \mathbf{0}.
\end{aligned}\right\} \quad \begin{aligned} n &= 1, 2, \ldots, N, \\ j &= 0, 1, 2, \ldots \end{aligned} \tag{25}$$

Substitution from (19)–(21) into (23)–(25) yields a non-standard infinite set of linear algebraic equations for the unknown coefficients $\mathbf{d}^{(n)}$, $\mathbf{v}^{(n)}$, $\mathbf{w}^{(n)}$, $\mathbf{q}_k^{(n)}$, $\mathbf{r}_k^{(n)}$, $\mathbf{s}_m^{(n)}$ and $\mathbf{t}_m^{(n)}$, ($n = 1, 2, \ldots, N$; $k = 1, 2, \ldots$; $m = 1, 2, \ldots$). A general theory for the resulting infinite system of equations does not exist. However, reasonably accurate solutions may be obtained by truncating the first and second series in (17) to K and $M^{(n)}$ terms, respectively. In this case, j is truncated to K integrations in (23) and (24) and $M^{(n)}$ integrations in (25). By equating the real and imaginary parts on both sides of these equations, we obtain a system of

$$12(KN + \sum_{n=1}^{N} M^{(n)} + N)$$

real equations in the same number of real unknowns. These equations when written as $\mathbf{Kc} = \mathbf{F}$ where $\mathbf{c}$ is the column vector of unknowns reveals that $\mathbf{K}$ is a sparse matrix. The choice of K and $M^{(n)}$ will determine the period of the largest harmonic in the set of basis functions on the surfaces $x_3^{(n)} = 0$, $h^{(n)}$ and $x_1^{(n)} = 0$, L, respectively. In order to maintain approximately the same period of the largest harmonic on all interfaces and boundaries, we choose

$$M^{(n)} = \text{Ceil}\left(K\frac{h^{(n)}}{L}\right), \tag{26}$$

where Ceil(y) gives the smallest integer greater than or equal to y. Thus the size of the matrix $\mathbf{K}$ will solely depend on the choice of K. Kantorovich and Krylov (1958) and Meleshko (1997) have discussed issues related to the solution of an infinite system of linear algebraic equations. The global system of equations needs to be modified when some or all components of the displacement are not prescribed anywhere on the boundary. Consider the case of a plate subjected to traction boundary condition on the top and bottom surfaces and boundary conditions on side surfaces specified by $\mathbf{I}_u^l = \mathbf{I}_u^r = \text{diag}[0, 1, 1]$. In this case the displacement u_1 is not specified on any part of the boundary. An example of such boundary conditions is a simply supported plate. The condition of static equilibrium requires that the first component of the prescribed loading satisfy

$$\int_0^L g_1^t(x_1)\,\mathrm{d}x_1 = \int_0^L g_1^b(x_1)\,\mathrm{d}x_1 + \sum_{n=1}^{N}\int_0^{h^{(n)}} [g_1^l(x_3^{(n)}) - g_1^r(x_3^{(n)})]\,\mathrm{d}x_3^{(n)}. \tag{27}$$

This condition in conjunction with the integral form of the equilibrium equations shows that the first component of the vector Eqs. (23)–(25) corresponding to $j = 0$ are linearly dependent. In order to obtain a unique solution to the problem, one of these equations has to be replaced by an equation that specifies the displacement u_1 at an arbitrary point in the domain, say $u_1(L/2, H/2) = 0$.

It should be noted from the structure of the solution (19)–(21) that the component functions decrease exponentially from the boundary/interfaces into the interior of the nth lamina. By truncating the series, we have effectively ignored coefficients with suffices greater than a particular value and approximated the coefficients which have small suffices. Due to the rapid decay of component functions associated with large suffices, the truncation of the series will not greatly influence the solution at the interior points. A larger value of K will give a more accurate solution at points close to the boundary and interfaces. It should also be noted that the coefficients $\mathbf{q}_k^{(n)}$ and $\mathbf{r}_k^{(n)}$ in (20)–(21) are multiplied by $\lambda_{k*}^{(n)}$ while $\mathbf{s}_m^{(n)}$ and $\mathbf{t}_m^{(n)}$ are multiplied by $\eta_{m*}^{(n)}$, thus indicating that the stresses will converge more slowly than the displacements.

Once the unknown coefficients are determined by satisfying the boundary and interface conditions, the displacements and stresses in each lamina are obtained from (19)–(21). Then the stress component σ_{22} missing in (20) and (21) is determined from (2). Nonzero values of coefficients $\mathbf{s}_m^{(n)}$ and $\mathbf{t}_m^{(n)}$ would indicate the existence of boundary layers near the edges of the laminate.

The solution of the problem could be singular at the four points where the top and bottom surfaces intersect the left and right edges, and also at points where the interfaces intersect the left and right edges $x_1 = 0, L$ (Ting, 1996). The asymptotic solution at these points can be analyzed by assuming $f_\alpha(z_\alpha)$ to be proportional to $z_\alpha^{\delta+1}$, where (x_1, x_3) is measured from the point and δ is an eigenvalue to be determined.

The stress is then proportional to z_α^δ. The satisfaction of the homogeneous boundary and interface conditions results in an eigenvalue problem for δ (Ting, 1996; Ting and Chou, 1981; Ting, 1986). The singular solution with an unknown multiplicative constant is then added to (17). When we attempted to determine the coefficients of the singular solutions by using the Least Squares method on the boundaries, the resulting set of linear equations became ill-conditioned and the coefficients behaved erratically as the number of terms in the series was increased. A similar problem was also encountered by Benthem (1963) when studying the deformations of a clamped semi-infinite strip loaded in tension. This difficulty was overcome by Gregory and Gladwell (1982) who used a projection method to incorporate the singular solution. The stress singularity and the stress intensity factor at the corners of a clamped plate have been evaluated by Tullini and Savoia (1995) by starting with an eigenvalue expansion of the edge problem. In the results discussed below, terms explicitly representing a singular solution have not been included.

5. Examples

For all the examples, we consider layers of unidirectional fiber reinforced material, model each layer as orthotropic and assign to it the following stiffness properties.

$$E_L/E_T = 25, \quad G_{LT}/E_T = 0.5, \quad G_{TT}/E_T = 0.2, \quad \nu_{LT} = \nu_{TT} = 0.25, \tag{28}$$

where E is the Young's modulus, G the shear modulus, ν the Poisson's ratio and subscripts L and T indicate, respectively, directions parallel and perpendicular to the fibers. Such properties are typical of a high modulus graphite-epoxy composite. For values given in (28) and fibers aligned along the x_1-direction, the nonzero components of the elasticity matrix C_{ijkl} are

$$C_{1111} = 25.168E_T, \quad C_{2222} = C_{3333} = 1.071E_T,$$

$$C_{1122} = C_{1133} = 0.336E_T, \quad C_{2233} = 0.271E_T,$$

$$C_{2323} = 0.2E_T, \quad C_{3131} = C_{1212} = 0.5E_T. \tag{29}$$

We choose $K = 400$ in order to obtain good accuracy close to the boundary and the interfaces.

We do not present results for simply supported orthotropic plates subjected to tractions on the top and bottom surfaces since they are identical to those of Pagano (1969). His solution reveals that the boundary and interface conditions can be satisfied by using only terms corresponding to k in (17). For a simply supported plate, coefficients $s_m^{(n)}$ and $t_m^{(n)}$ are found to be zero. As pointed out above, the vanishing of these coefficients implies the absence of boundary layers near the edges of a simply supported orthotropic plate. In such cases, the infinite system of Eqs. (23)–(25) will be uncoupled for each j. Thus the solution for the infinite system is obtained by solving a finite system for each j. This explains why it is 'easier' to obtain a solution for simply supported edges than when the edges are clamped.

5.1. Clamped-clamped laminate

The first example concerns a single layered homogeneous composite plate, clamped on both the side surfaces $x_1 = 0, L$ and subjected to traction boundary condition on the top and bottom surfaces. The fibers are along the x_1 direction. The following sinusoidal distribution of traction is applied on the top surface while the bottom surface is traction free
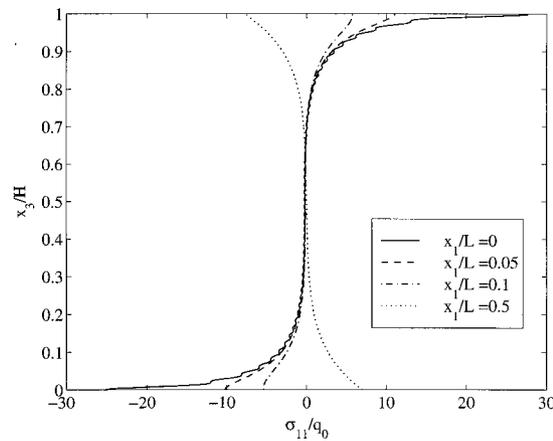
Fig. 2. Longitudinal stress distribution on four sections for a clamped-clamped homogeneous plate ($L/H = 4$).

$$\mathbf{g}^{\mathrm{t}}(x_1) = q_0 \left[0, \, 0, \, -\sin \frac{\pi x_1}{L} \right]^{\mathrm{T}}, \quad \mathbf{g}^{\mathrm{b}}(x_1) = \mathbf{0}. \tag{30}$$

Figs. 2 and 3 show the distribution of the longitudinal and transverse shear stress over the thickness of a thick laminate with $L/H = 4$, where H equals the thickness of the laminate. The oscillatory behavior of the stresses observed at the clamped surface is due to the truncation of the series and the slow convergence of the stresses close to the boundaries. The amplitude of the oscillation decreases when K is increased. The magnitude of the longitudinal stress on the top surface at points away from the clamped edges is slightly higher than that at corresponding points on the bottom surface. Right at the corners of the clamped edges, the longitudinal stress is finite because of the truncation of the infinite series. As shown by Tullini and Savoia (1995) and Gregory and Gladwell (1982), the longitudinal stress at the corners of a clamped end is unbounded. If we disregard the oscillations, due to the Gibbs phenomenon, in
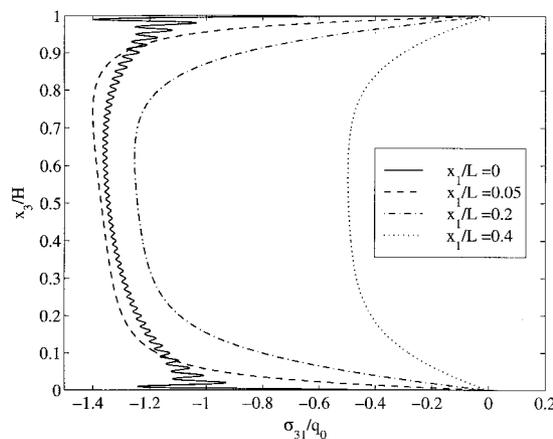
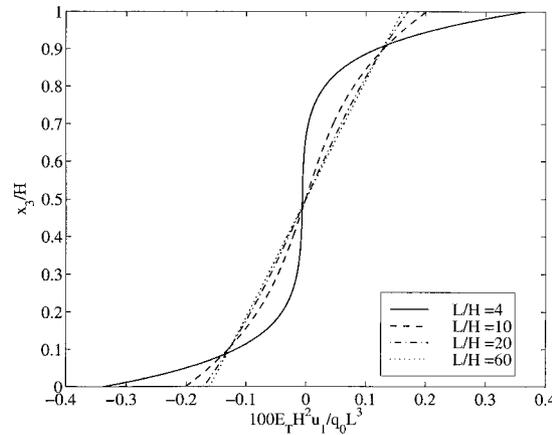Fig. 3. Transverse shear stress distribution on four sections for a clamped-clamped homogeneous plate ($L/H = 4$).

Fig. 4. Axial displacement distribution on the section $x_1 = L/4$ for a clamped-clamped homogeneous plate for four values of L/H.

the values of σ_{31} at points on $x_1/L = 0$, or 1, then the absolute value of the transverse shear stress attains its maximum at a point in the upper half of the plate. This asymmetry in the stresses can be attributed to the external loading being applied to the top surface while the bottom surface is traction free. At the clamped ends the transverse shear stress is almost uniform through the thickness of the plate. The thicknesses of the boundary layers at the top and bottom surfaces decrease with an increase in the distance of the cross-section from the midplane.

The classical laminated plate theory (CLPT) solution for the transverse displacement $\tilde{u}_3$ and the longitudinal stress $\tilde{\sigma}_{11}$ is

$$\tilde{u}_3(x_1, x_3) = -\frac{12(1 - \nu_{LT}\nu_{TL})q_0 L^4}{25 E_T H^3 \pi^4}\left[\pi\frac{x_1}{L}\left(\frac{x_1}{L} - 1\right) + \sin\frac{\pi x_1}{L}\right], \quad \nu_{TL} = \nu_{LT}E_T/E_L,$$
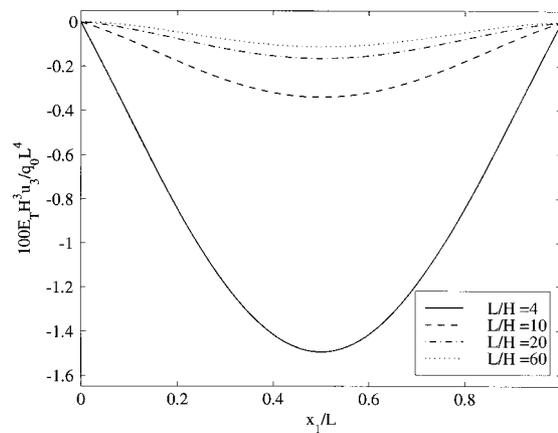
Fig. 5. Deflected shapes of the mid-surface of a clamped-clamped homogeneous plate for four values of L/H.

Table 1
Transverse deflection, longitudinal stress, transverse shear stress, transverse normal stress and extension of the normal for increasing span-to-thickness ratios

$\frac{L}{H}$	$\frac{100E_T H^3}{q_0 L^4} u_3(\frac{L}{2}, \frac{H}{2})$	$\frac{H^2}{q_0 L^2} \sigma_{11}(\frac{L}{2}, H)$	$\frac{H}{q_0 L} \sigma_{31}(\frac{L}{4}, \frac{H}{2})$	$\frac{1}{q_0} \sigma_{33}(\frac{L}{2}, \frac{H}{2})$	$\frac{10 E_T}{q_0 H}[u_3(\frac{L}{2}, H) - u_3(\frac{L}{2}, 0)]$
4	−1.4946	−0.4887	−0.2765	−0.490	−4.6238
6	−0.7412	−0.3532	−0.3011	−0.497	−4.6608
8	−0.4688	−0.2987	−0.3160	−0.499	−4.6701
10	−0.3402	−0.2716	−0.3246	−0.500	−4.6731
15	−0.2111	−0.2437	−0.3333	−0.500	−4.6747
20	−0.1652	−0.2338	−0.3356	−0.500	−4.6750
30	−0.1322	−0.2266	−0.3368	−0.500	−4.6750
40	−0.1205	−0.2241	−0.3372	−0.500	−4.6750
60	−0.1122	−0.2223	−0.3374	−0.500	−4.6750
CLPT	−0.1055	−0.2209	−0.3376	−0.500	–

$$\tilde{\sigma}_{11}(x_1, x_3) = \frac{12 q_0 L^2}{H^2 \pi^3}\left(2 - \pi \, \sin \frac{\pi x_1}{L}\right)\left(\frac{x_3}{H} - \frac{1}{2}\right).$$

The transverse shear and normal stresses are assumed to be zero in the CLPT; however they may be computed by integrating the three-dimensional equilibrium equations of elasticity after $\tilde{\sigma}_{11}$, $\tilde{\sigma}_{22}$ and $\tilde{\sigma}_{12}$ have been found. The transverse stresses thus obtained are

$$\tilde{\sigma}_{13}(x_1, x_3) = -\frac{6 L q_0}{\pi H}\left(\frac{x_3}{H} - \frac{x_3^2}{H^2}\right)\cos \frac{\pi x_1}{L},$$

$$\tilde{\sigma}_{33}(x_1, x_3) = -\frac{q_0 x_3^2}{H^2}\left(3 - \frac{2 x_3}{H}\right)\sin \frac{\pi x_1}{L}.$$

The through-thickness variation of the normalized displacement u_1 plotted in Fig. 4 shows an affine variation for span-to-depth ratios of 20 or more. The normalized midplane lateral displacement u_3 (cf. Fig. 5) shows that for large span-to-depth ratios the slope of the deformed midplane at the clamped edge
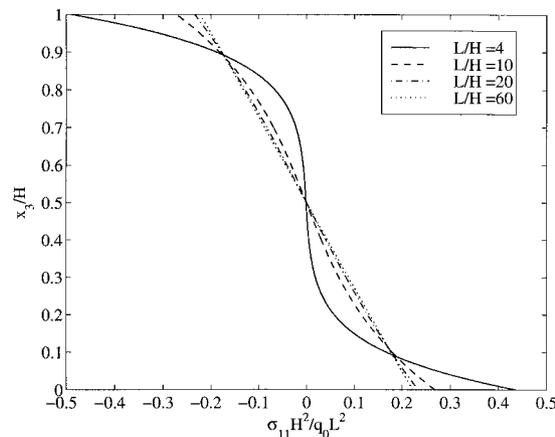

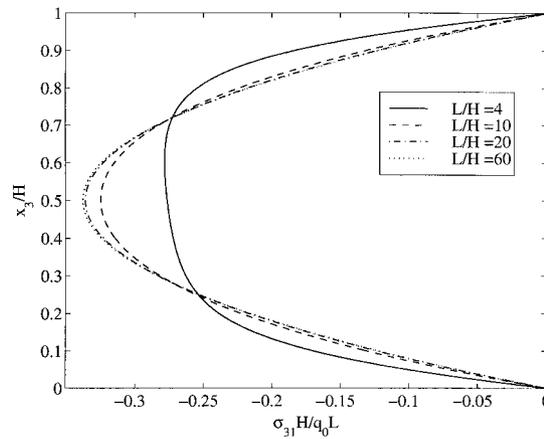Fig. 6. Normal stress distribution at $x_1 = L/2$ for a clamped-clamped homogeneous plate for four values of L/H.

Fig. 7. Transverse shear stress distribution at $x_1 = L/4$ for a clamped-clamped homogeneous plate for four values of L/H.

approaches zero. These results support the assumptions of laminated plate theories for thin plates. For thick plates the slope at the clamped edge is no longer small due to the effect of transverse shear deformation. Note that the CLPT predicts the normalized midplane lateral displacement at the plate centroid to be -0.1055 for all values of L/H. Table 1 lists, for various span-to-thickness ratios, the numerical values of normalized transverse deflection u_3 at the center of the plate, the normalized longitudinal stress at $(L/2, H)$, the nondimensional transverse shear stress at $(L/4, H/2)$, the nondimensional transverse normal stress at $(L/2, H/2)$ and the normalized elongation of the normal to the midsurface of the plate. For thin plates the transverse deflection and values of the stress components asymptotically approach those given by the CLPT theory. These results are similar to those of Pagano (1969) for simply supported laminated plates. The classical beam and thin plate theories assume inextensibility in the transverse direction; e.g. see Reddy (1997), Jones (1975). Table 1 and results plotted in Figs. 4 and 5 also reveal that the elongation of the normal at the mid-span is $O(q_0 H/E_T)$ and the displacements u_1 and u_3 are $O(q_0 L^3/E_T H^2)$ and $O(q_0 L^4/E_T H^3)$, respectively. Figs. 6 and 7 show that the through-thickness normal and shear stresses approach the affine and parabolic distributions predicted by the CLPT as $L/H \to \infty$.
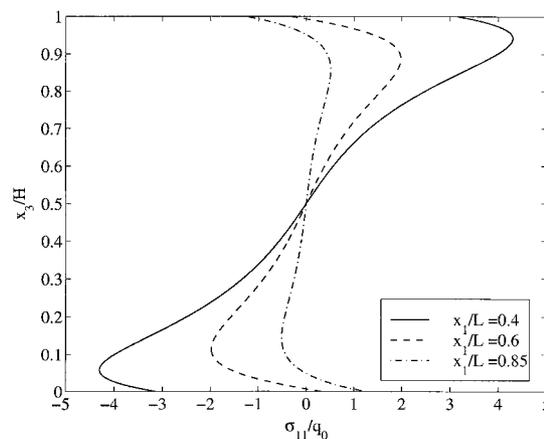

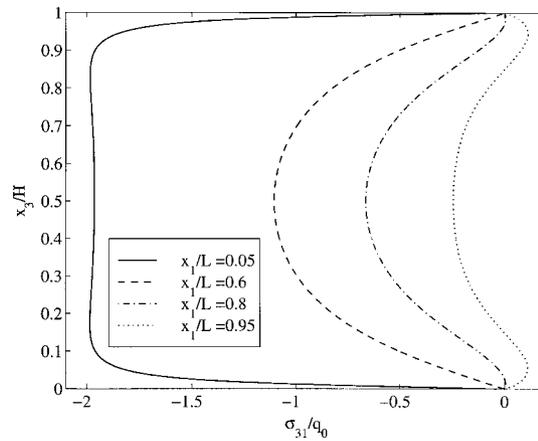Fig. 8. Normal stress distribution on three sections for a cantilever homogeneous plate ($L/H = 2$).

Fig. 9. Transverse shear stress distribution on four sections for a cantilever homogeneous plate ($L/H = 2$).

Soldatos and Watson (1997) have attempted to solve the same problem with an improved higher order theory. Their theory incorporates the through-thickness shape functions obtained from the exact solution of the corresponding simply supported plate. The boundary conditions on the edges are applied in an average sense like in other plate theories. These boundary conditions lead to inaccurate stress distributions at the clamped edges. At the edge $x_1 = 0$, their approximate solution yields a positive value for the shear stress on the lower half of the plate and regions of highly negative normal stresses in the upper half, in contrast to our results. Similarly, their results do not compare well with our through-thickness distributions for the displacement u_1 at any location along the span.

5.2. Cantilever laminate

We study deformations of a single layered homogeneous cantilever plate clamped at the surface $x_1 = 0$, traction free at $x_1 = L$, and subjected to uniform normal loads on the top and bottom surfaces given by $g_3^t(x_1) = -q_0/2$, $g_3^b(x_1) = q_0/2$. The fibers are aligned along the x_1 direction. The span to thickness ratio,
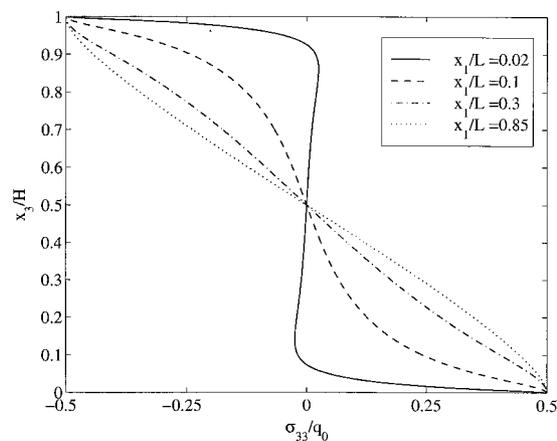

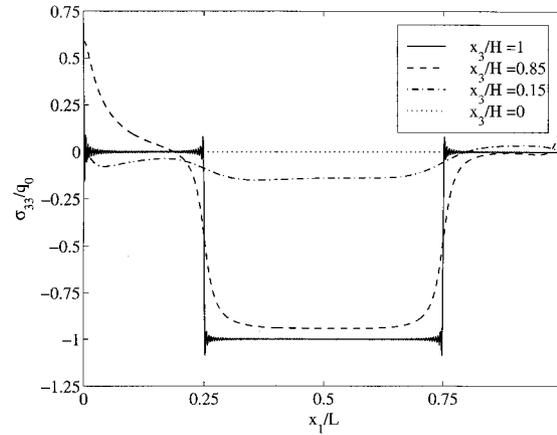Fig. 10. Transverse normal stress distribution on four sections for a cantilever homogeneous plate ($L/H = 2$).

Fig. 11. Variation on four planes of transverse normal stress for a clamped-simply supported three-layer laminate.

L/H, is taken as 2, which characterizes a very thick plate. The through-thickness distribution of the longitudinal stress and the transverse shear stress shown in Figs. 8 and 9 agree qualitatively with the results of Savoia and Tullini (1996). Their theory is based on the assumptions of transverse inextensibility and plane stress. They have also compared their results with that obtained by the Finite Element Analysis. Their results for the transverse normal stress σ_{33} are inaccurate due to the assumption of transverse inextensibility while the distributions shown in Fig. 10 are in agreement with those obtained by the Finite Element Analysis under the assumption of plane strain deformations. It is clear from the results plotted in Fig. 9 that near the free end, $x_1/L = 0.95$, the sign of the transverse shear stress at points near the top and bottom surfaces is opposite of that given by the classical beam theory which is not expected to give good results for span to thickness ratio of 2.

Near the clamped edge, the transverse normal stress exhibits boundary layer effects adjacent to the top and bottom surfaces and is essentially negligible through most of the thickness.

5.3. Clamped-simply supported laminate

The final example concerns a three-layer composite laminate. The orientations of the fibers with respect to the x_1 axis are $0°$, $90°$ and $-45°$ in the lower, middle and top layers respectively. The thicknesses of the three layers are

$$[h^{(1)}, h^{(2)}, h^{(3)}] = [0.3, 0.4, 0.3]H, \quad \text{and} \quad L/H = 5. \tag{31}$$

The surface $x_1 = 0$ is clamped while the surface $x_1 = L$ is simply supported. The top surface is subjected to a discontinuous normal traction and the bottom surface to a constant shear traction given by

$$\mathbf{g}^{t}(x_1) = q_0 \left[0, 0, -\mathcal{H}\left(x_1 - \frac{L}{4}\right) + \mathcal{H}\left(x_1 - \frac{3L}{4}\right) \right]^{\mathrm{T}},$$

$$\mathbf{g}^{b}(x_1) = q_0 \left[-0.5, 0, 0\right]^{\mathrm{T}}, \tag{32}$$

where $\mathcal{H}$ is the Heaviside step function. The highly anisotropic nature of the material, the small value
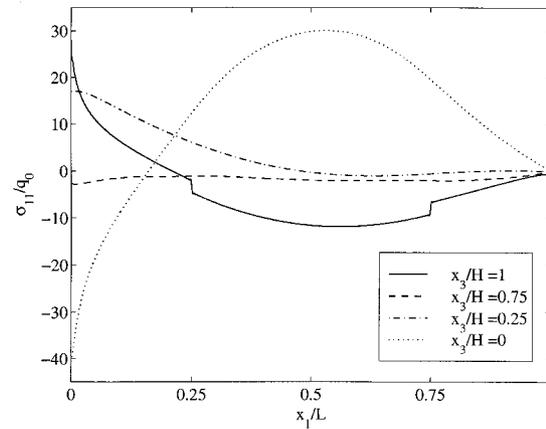
Fig. 12. Variation of longitudinal stress on four planes for a clamped-simply supported three-layer laminate.

of L/H for the plate, and the discontinuous traction on the top surface in conjunction with the clamped boundary condition are considered a severe test of the reliability of the present method.

The distribution of the transverse normal stress, on different horizontal planes, shown in Fig. 11 indicates that the traction boundary conditions on the top and bottom surfaces are well satisfied. One sees Gibbs phenomenon near the clamped end, and at points where the prescribed traction distribution is discontinuous. The distribution of the longitudinal stress on horizontal planes $x_3/H = 1$, 0.75, 0.25 and 0 plotted in Fig. 12 depicts the familiar boundary layer on the top and bottom surfaces at the clamped edge. It also exhibits jumps on the top surface at $x_1 = L/4$, and $3L/4$ which are points of discontinuity of the prescribed transverse normal traction. The through thickness distributions of the longitudinal stress σ_{11} are shown in Fig. 13. The distribution of the longitudinal stress on horizontal planes equidistant from the midsurface is not symmetrical. On the top surface the longitudinal stress is discontinuous at the two points where the applied normal traction jumps from zero to a finite value, but on the bottom surface it is continuous. The shear stress distributions are shown in Figs. 14 and 15, and Fig. 16 gives
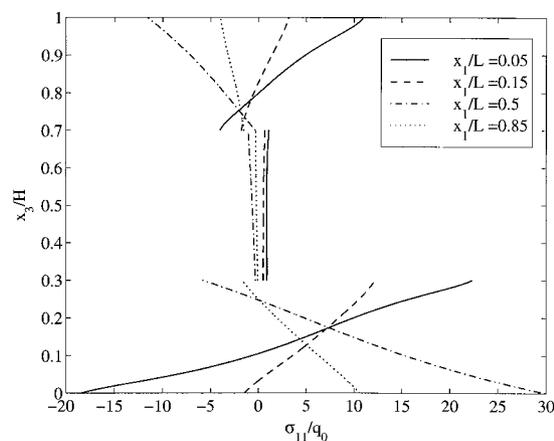

Fig. 13. Distribution of the longitudinal stress on four sections for a clamped-simply supported three-layer laminate.
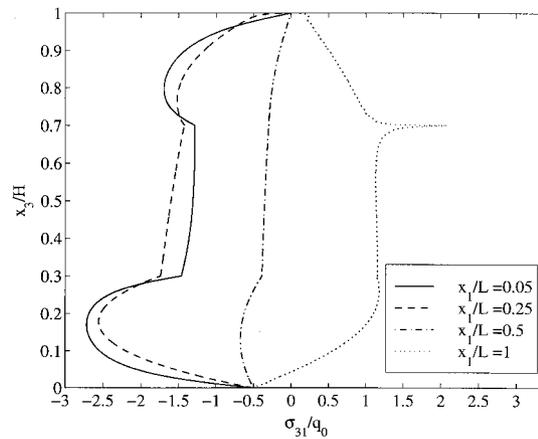
Fig. 14. Transverse shear stress distribution on four sections for a clamped-simply supported three-layer laminate.

the through-thickness distributions of the axial displacement at four sections. The results plotted in these figures clearly show that the boundary and interface conditions are very well satisfied. The different orientations of the fibers near the top and bottom surfaces strongly influence the through-thickness distribution of the longitudinal and transverse shear stresses.

6. Conclusions

We have used the Eshelby–Stroh formalism to study the generalized plane strain quasistatic deformations of a linear elastic anisotropic laminated plate with either both edges clamped or one edge clamped and the other simply supported or one edge clamped and the other free. The three-dimensional equations of elastostatics are exactly satisfied at every point of the body. However, the boundary and interface continuity conditions are satisfied in the sense of Fourier series. When sufficient (400) terms are kept in the analytical series solution, these boundary and interface continuity conditions are also well
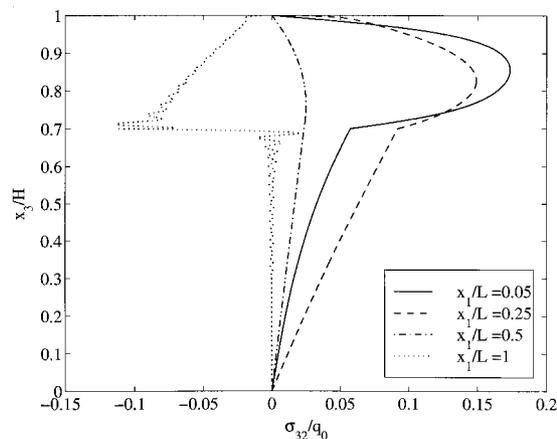

Fig. 15. Distribution of transverse shear stress σ_{32} on four sections for a clamped-simply supported three-layer laminate.
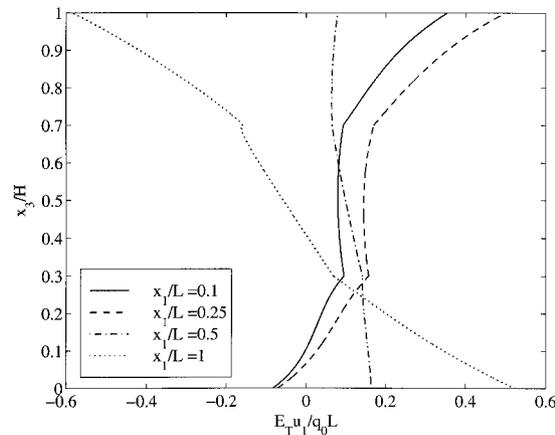
Fig. 16. Distribution of the axial displacement on four sections for a clamped-simply supported three-layer laminate.

satisfied at every point on these surfaces. The solution is valid for all aspect ratios of the plate, and exhibits boundary layers near the clamped edges, top and bottom surfaces and interfaces between different layers. It is found that even for a single layer orthotropic plate with span to thickness ratio of 10, the slope of deformed midplane is nonzero at the clamped edges. For a distributed transverse load applied on the top surface of the plate, the longitudinal and transverse shear stresses are found to be asymmetric about the midsurface of the plate. Also, the change in the plate thickness at the midspan is of the order of $q_0 H / E_T$ where q_0 is the intensity of the distributed load, H the initial thickness of the plate and E_T the transverse modulus. Only for thin plates, the through thickness variation of the longitudinal stress is affine and that of the transverse shear stress parabolic. Our results for thin plates agree with those of the classical laminated plate theory.

For a cantilever plate with span to thickness ratio of two and loaded by uniformly distributed loads of the same intensity on the top and bottom surfaces, the through-thickness distribution of the transverse shear stress is parabolic at sections near the midspan. At sections near the free end, the sign of the transverse shear stress near the top and bottom surfaces is opposite of that near the midsurface; the latter is of the same sign as that given by the classical beam theory. On a section close to the clamped end the transverse shear stress is nearly uniform through the thickness except at points in the vicinity of the top and bottom surfaces where it exhibits a boundary layer effect. At the section adjacent to the clamped end, the transverse normal stress also shows a boundary layer effect, is almost zero through most of the thickness, and approaches the prescribed value at the top and bottom surfaces.

We have also computed stresses and displacements in a composite plate of span to thickness ratio equal to 5, clamped at one end and simply supported at the other end, and loaded by a uniformly distributed transverse load on a part of the upper surface and uniformly distributed tangential tractions on the lower surface. The computed results show that the transverse shear stresses are continuous at the interfaces between adjoining laminae, and the traction boundary conditions are well satisfied on the top and bottom surfaces. Because of the different boundary conditions on the two edges, the deformations of plane sections perpendicular to the midsurface of the plate and located symmetrically about the midspan are different. Also, the different orientation of fibers near the top and bottom surfaces strongly influences the through-thickness variation of the transverse shear stresses.

The results presented herein should help check the validity of various approximate plate theories.

Acknowledgements

References

Benthem, J.P., 1963. A Laplace transform method for the solution of semi-infinite and finite strip problems in stress analysis. The Quarterly Journal of Mechanics and Applied Mathematics 16, 413–429.

Eshelby, J.D., Read, W.T., Shockley, W., 1953. Anisotropic elasticity with applications to dislocation theory. Acta Metallurgica 1, 251–259.

Jones, R.M., 1975. Mechanics of Composite Materials. Scripta Book Co, Washington, DC.

Gregory, R.D., Gladwell, I., 1982. The cantilever beam under tension, bending or flexure at infinity. Journal of Elasticity 12, 317–343.

Kantorovich, L.V., Krylov, V.I., 1958. Approximate Methods of Higher Analysis. P. Noordhoff, Groningen, The Netherlands.

Kapania, R.K., Raciti, S., 1989. Recent advances in analysis of laminated beams and plates, Part I: Shear effects and buckling. AIAA Journal 27, 923–934.

Meleshko, V.V., 1997. Bending of an elastic rectangular clamped plate: exact versus 'engineering' solutions. Journal of Elasticity 48, 1–50.

Noor, A.K., Burton, W.S., 1989. Assessment of shear deformation theories for multilayered composite plates. Applied Mechanics Reviews 42, 1–13.

Pagano, N.J., 1969. Exact solutions for composite laminates in cylindrical bending. Journal of Composite Materials 3, 398–411.

Pagano, N.J., 1970. Influence of shear coupling in cylindrical bending of anisotropic laminates. Journal of Composite Materials 4, 330–343.

Reddy, J.N., 1997. Mechanics of Laminated Composite Plates: Theory and Analysis. CRC Press, Boca Raton, FL.

Savoia, M., Tullini, N., 1996. Beam theory for strongly orthotropic materials. International Journal of Solids and Structures 33, 2459–2484.

Soldatos, K.P., Watson, P., 1997. Accurate stress analysis of laminated plates combining a two-dimensional theory with the exact three-dimensional solution for simply supported plates. Mathematics and Mechanics of Solids 2, 459–489.

Srinivas, S., Rao, A.K., 1973. Flexure of thick rectangular plates. Journal of Applied Mechanics 40, 298–299.

Stroh, A.N., 1958. Dislocations and cracks in anisotropic elasticity. Philosophical Magazine 3, 625–646.

Ting, T.C.T., 1996. Anisotropic Elasticity. Theory and Applications. Oxford University Press, New York Oxford Engineering Science Series.

Ting, T.C.T., 1986. Explicit solution and invariance of the singularities at an interface crack in anisotropic composites. International Journal of Solids and Structures 22, 965–983.

Ting, T.C.T., 1982. Effects of change of reference coordinates on the stress analyses of anisotropic elastic materials. International Journal of Solids and Structures 18, 139–152.

Ting, T.C.T., Chou, S.C., 1981. Edge singularities in anisotropic composites. International Journal of Solids and Structures 17, 1057–1068.

Tullini, N., Savoia, M., 1995. Logarithmic stress singularities at clamped-free corners of a cantilever orthotropic beam under flexure. Composites Structures 32, 659–666.